Quantized Electron Accumulation States in Indium Nitride Studied by Angle-Resolved Photoemission Spectroscopy

Leyla Colakerol,[1] T. D. Veal,[2] Hae-Kyung Jeong,[1] Lukasz Plucinski,[1] Alex DeMasi,[1] Timothy Learmonth,[1] Per-Anders Glans,[1] Shancai Wang,[1] Yufeng Zhang,[1] L. F. J. Piper,[2] P. H. Jefferson,[2] Alexei Fedorov,[3] Tai-Chou Chen,[4] T. D. Moustakas,[4] C. F. McConville,[2] and Kevin E. Smith[1,*]

[1]*Department of Physics, Boston University, Boston, Massachusetts 02215, USA*
[2]*Department of Physics, University of Warwick, Coventry, CV4 7AL, United Kingdom*
[3]*Advanced Light Source, Lawrence Berkeley National Laboratory, Berkeley, California 94720, USA*
[4]*Department of Electrical and Computer Engineering, Boston University, Boston, Massachusetts 02215, USA*

(Received 16 June 2006; published 4 December 2006)

Electron accumulation states in InN have been measured using high resolution angle-resolved photoemission spectroscopy (ARPES). The electrons in the accumulation layer have been discovered to reside in quantum well states. ARPES was also used to measure the Fermi surface of these quantum well states, as well as their constant binding energy contours below the Fermi level E_F. The energy of the Fermi level and the size of the Fermi surface for these quantum well states could be controlled by varying the method of surface preparation. This is the first unambiguous observation that electrons in the InN accumulation layer are quantized and the first time the Fermi surface associated with such states has been measured.

DOI: 10.1103/PhysRevLett.97.237601 PACS numbers: 79.60.Bm, 71.18.+y, 71.20.Nr, 73.20.At

Group III-nitride semiconductors have been the subject of intense scrutiny for many years due to their use in optoelectronic devices operating in the blue and UV range of the electromagnetic spectrum [1]. Much recent attention has focused on InN, where, due to improved film growth methods, the energy of the fundamental band gap has undergone a remarkable revision in the last five years from the previously accepted value of approximately 1.9 eV to the much lower value of approximately 0.65 eV [2]. The band gap of the $In_xGa_{1-x}N$ ternary alloy system now spans the near infrared to the UV, enabling the entire optical window to be encompassed by a single material system [3].

InN is unusual in that there is strong experimental evidence for the existence of an intrinsic electron accumulation layer near the surface of the thin films. It is postulated that the surface region has a higher charge density than the bulk due to N vacancies or donor-type surface states. This causes the surface Fermi level to lie in the conduction band. The conduction band minimum (CBM) is at the Brillouin zone center (Γ) in InN [4]. It is formed by a rapidly dispersing band, resulting in the CBM lying at a significantly lower energy than the momentum averaged conduction band edge, as visible in the calculated band structure [4]. Evidence for an accumulation layer comes from high resolution electron energy loss spectroscopy studies [4,5], which revealed a conduction band plasmon whose energy increased as the incident electron energy was reduced, indicating a higher electron density within 80 Å of the surface than in the bulk. Further evidence comes from sheet carrier density measurements as a function of film thickness, capacitance-voltage measurements, a photoemission study of defective InN coated with Ti [6,7], and recent tunneling spectroscopy experiments [8].

We report here the direct observation of electron accumulation in InN using high resolution angle-resolved photoemission spectroscopy (ARPES). Not only are electrons observed far above the CBM, but these electrons are found to be quantized perpendicular to the surface; i.e., the electrons in the accumulation layer have been determined to reside in quantum well states. ARPES was also used to measure the Fermi surface of the quantum well states, as well as their constant binding energy contours below the Fermi level E_F. The Fermi surface was found to consist of concentric, perfectly circular structures associated with each of two quantum well states, but the corresponding energy contours assume a hexagonal symmetry away from E_F. The Fermi level and the size of the Fermi surface for these quantum well states could be controlled by varying the method of surface preparation. This is the first unambiguous observation that electrons in the InN accumulation layer are quantized and the first time the Fermi surface associated with such states has been measured.

The experiments were undertaken on beam line U5UA at the National Synchrotron Light Source (NSLS), Brookhaven National Laboratory, and on beam line 12.0.1 at the Advanced Light Source (ALS), Lawrence Berkeley National Laboratory. Both beam lines are equipped with 100 mm hemispherical electron energy analyzers (Scienta SES100). Typical energy and full angular resolution were 60 meV and 1°, respectively, for the instrument on U5UA, and 35 meV and 0.5° for the instrument on BL 12.0.1. The InN films were grown on *c*-plane sapphire substrates by radio frequency plasma-assisted molecular beam epitaxy [9]. The films are autodoped *n* type with an average carrier concentration 5×10^{19} cm^{-3} and an average electron mobility 340 cm^2/V · s. The room temperature optical gap was approximately 0.77 eV as

determined by the peak of the derivative of the absorption constant [9]; this is consistent with the fundamental energy band gap of 0.65 eV [2,10]; i.e., there is a Moss-Burstein shift of the optical absorption to higher energy due to degenerate doping [2]. As will be discussed below, samples were cleaned by annealing in ultrahigh vacuum (UHV), or by cycles of 500 eV N_2^+ ion bombardment followed by annealing in UHV. All surfaces exhibited sharp 1×1 low-energy electron diffraction (LEED) patterns with a low background. ARPES spectra were recorded with the sample at 177 K for experiments at U5UA and 60 K for experiments at BL 12.0.1. Binding energies are referenced to E_F, determined from a Au foil in contact with the sample.

Figure 1 presents a series of ARPES spectra from InN. In Fig. 1(a), the photon energy is swept from 51 to 92 eV, and the spectra recorded in a normal emission mode, probing states along the ΓΔA direction in the bulk Brillouin zone. The surface in this case was processed by annealing the film to 400 °C in UHV. In Fig. 1(b), the photon energy and angle of emission are varied in order to measure states along the ΓTK direction. This is parallel to the film surface. The sample in this case was processed by annealing to 500 °C in UHV. The energy distribution curves (EDCs) in Fig. 1 are plotted relative to E_F. It is immediately clear that two discrete photoemission features are observed at binding energies near E_F for photon energies between 63 and 79 eV, and that they appear only for a narrow cone of emission angles (θ) around the normal ($\pm$ 2.5° for $h\nu =$ 69 eV). The leading edge of the main valence band emission feature lies 1 eV ($\pm$ 0.05 eV) below E_F. This is consistent with significant band bending near the surface.

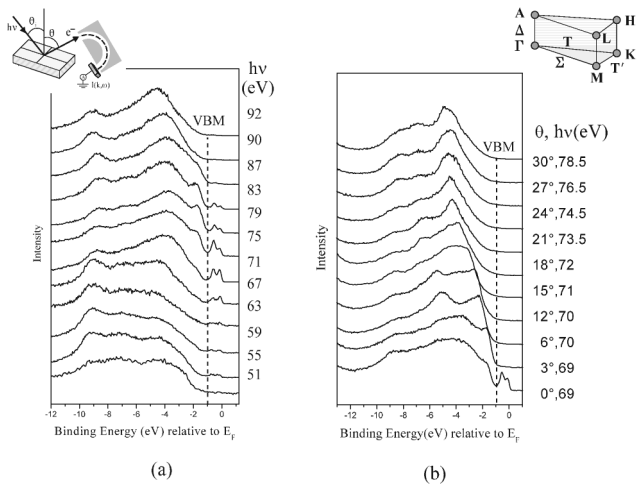

FIG. 1. ARPES spectra from InN. (a) Series of normal emission spectra ($\theta = 0°$) for $h\nu$ from 51 to 92 eV. (b) Series of spectra where $h\nu$ and θ are simultaneously varied to measure states along the ΓTK direction (parallel to the film surface) in the bulk Brillouin zone. Sample was annealed to 400 °C in UHV for (a) and 500 °C for (b). Spectra were recorded with the sample at room temperature. Inset: experimental geometry ($\theta_i = 45°$ in all cases), and symmetry labels for the bulk Brillouin zone.

This is neither the energy of the bulk valence band maximum (VBM) nor that of the VBM at the vacuum interface, rather it is the VBM at some finite depth away from the surface. Nevertheless, given the magnitude of the bulk band gap, the two discrete features close to E_F must originate from electrons in the conduction band. The narrow range of emission angles over which these features are observed indicates that the emitting states are highly localized in k space. These are not surface states, since exposure of the surface to atomic hydrogen did not remove these emission features. The features below the VBM originate primarily from bulk InN states; detailed analysis of these states will be presented elsewhere. ARPES has been used previously to measure states due to electron accumulation in InAs [11], but no unambiguous evidence for the quantized nature of such states was reported.

High resolution ARPES spectra were recorded for the energy range between E_F and the VBM. Figure 2 presents an ARPES photocurrent intensity map of emission from the states within 1.5 eV of E_F, recorded with an incident photon energy of 69 eV, from a sample annealed in UHV to 300 °C for 30 min. The sample was held at 177 K during measurement. The horizontal axis is the angle of emission, converted to momentum at each point, while the vertical axis is the binding energy; the intensity reflects the photocurrent for any particular binding energy and momentum. The momentum direction is along ΓΣM, in the surface plane. Two well-resolved, nested bands are observed. These states are symmetric around Γ, and determine E_F. The measured separation between the top of the valence band emission and E_F is 1.2 eV for this surface.

Figure 3(a) presents an ARPES intensity map from a sample that was treated with two cycles of 500 eV N_2^+ ion bombardment (10 min) and annealing in UHV to 300 °C (10 min). The incident photon energy was 70 eV, and the sample was held at 60 K during measurement. As in Fig. 2,

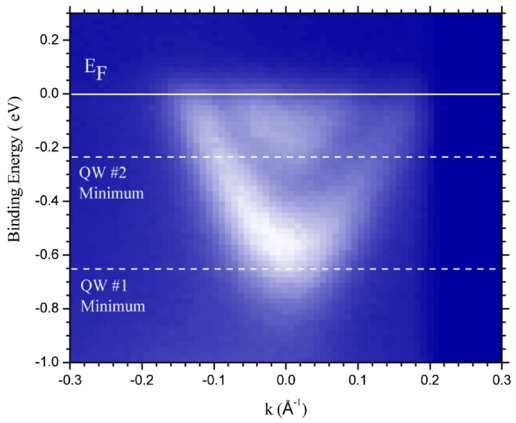

FIG. 2 (color online). ARPES photocurrent intensity map of states within 1.5 eV of E_F. $h\nu = 69$ eV and sample temperature was 177 K. Sample was annealed to 300 °C in UHV for 30 min. The false color intensity reflects the photocurrent, with lighter intensity indicating higher current. The momentum direction is along ΓΣM, in the surface plane.

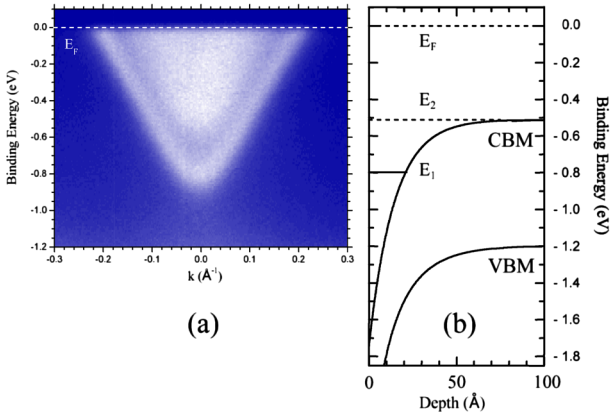

FIG. 3 (color online). (a) ARPES photocurrent intensity map of states within 1.2 eV of E_F. $h\nu = 70$ eV, and sample temperature was 60 K. Sample was prepared by two cycles of 500 eV Ar^+ ion bombardment and annealing in UHV to 300 °C (10 min for each ion bombardment and annealing step). The momentum direction is the same as in Fig. 2. (b) The calculated downward bending of the CBM and VBM (solid black curves) with respect to E_F. Optimum agreement between calculations and the experimental data was obtained using a bulk free electron density of $4 \times 10^{19}\,\mathrm{cm}^{-3}$ and band bending of 1.3 eV. An exponential approximation to the surface potential well is also shown with the corresponding subband minima, E_1 and E_2 at 0.511 and 0.797 eV, respectively.

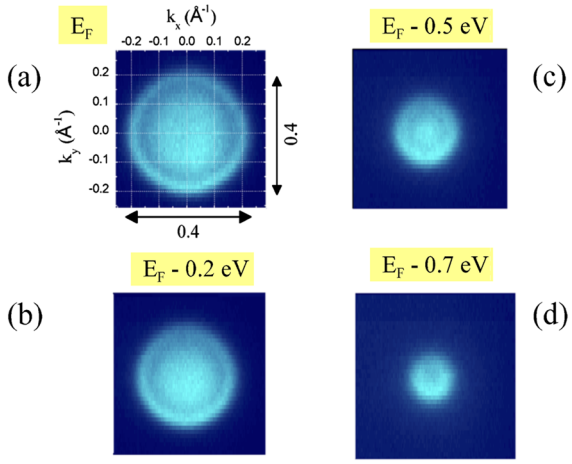

FIG. 4 (color online). Fermi surface and constant binding energy contours extracted from the data of Fig. 3. The photocurrent is plotted as k_x and k_y are varied, while the binding energy relative to E_F is kept constant at 0 (Fermi surface), 0.2, 0.5, and 0.7 eV. $h\nu = 70$ eV and sample temperature was 60 K. The diameter of the outer Fermi surface is 0.4 Å^{-1}.

the dispersive direction is along ΓΣM. Two well-resolved, nested bands are again observed. However, now the measured separation between the top of the valence band emission and E_F is 1.45 eV. This indicates that there is far more charge in the conduction band for this surface, compared to when the surface is prepared by annealing alone. Figure 3(b) presents the results of a calculation of the valence and conduction band bending, and the quantum well subband minima; this calculation is discussed below.

Figure 4 presents a series of constant binding energy photocurrent intensity contours extracted from the same data set as in Fig. 3(a). Contours are plotted for binding energies of (a) 0, (b) 0.2, (c) 0.5, and (d) 0.7 eV, relative to E_F. The 0 eV binding energy contour in Fig. 4(a) corresponds to the Fermi surface, which consists of two well-defined concentric structures that are perfectly circular, and centered around the surface normal. The diameter of the outer Fermi surface is 0.4 Å^{-1}. Note that the band forming the outer Fermi surface is well defined, but the emission from the inner band is quite diffuse. As the binding energy increases away from E_F, a hexagonal structure appears in the contours. This is most clearly seen in Fig. 4(c).

The spectra in Figs. 1–3 are direct evidence for quantum well states in the accumulation layer in InN. Band structure calculations show that there is only one bulk conduction band state near the Γ point [4]. The first question to address is why we see *two* states above the valence band emission in the ARPES experiment. These states, although derived from the conduction band, arise from the existence of a potential well perpendicular to the film surface. Downward band bending forms a one-dimensional (1D) potential well and the resulting two dimensional (2D) electron gas is quantized along the surface normal. This band bending is the result of donor-type surface states or N vacancies pinning E_F above the CBM [6,12].

The two states that we observe exhibit quantum well characteristics perpendicular to the surface, but have the characteristics of the conduction band in the plane parallel to the surface. As can be seen most clearly in Fig. 3, the dispersion of the states is not parabolic. Rather, it is linear away from the subband minima, and mimics the calculated dispersion of the conduction band along this direction [4]. The band bending calculated by solving the Poisson equation within the modified Thomas-Fermi approximation (MTFA) [13], including the effects of conduction band nonparabolicity [14], is shown in Fig. 3(b). The surface potential well obtained from the Poisson-MTFA method can be approximated by an exponential form. The 1D independent electron Schrödinger equation can then be solved analytically [8,15]. Using a bulk free electron density of 4×10^{19} cm^{-3} and a band bending of 1.25 eV, corresponding to a surface sheet density of 5.9×10^{13} cm^{-2}, these calculations predict the existence of two subbands with minima at 0.511 and 0.797 eV below E_F, with associated electron effective masses of $0.12m_0$ and $0.161m_0$, respectively. As can be seen in Fig. 3, the agreement between the calculated and measured subband minima is excellent. Our estimated surface charge density falls within the range of values determined by other techniques, 2×10^{13} to 3×10^{14} cm^{-2} [5,6,16].

The next question to address is the origin of the difference between the spectra in Figs. 2 and 3. The spectra in Fig. 3 were recorded at a lower temperature, and with a higher instrumental resolution, leading to sharper features and more clearly visible nonparabolic dispersion of the

TABLE I. Calculated characteristic parameters for InN. See text for details.

Parameter	Figure 2 data	Figure 3 data
Temperature	177 K	60 K
Bulk free electron density	6×10^{18} cm^{-3}	4×10^{19} cm^{-3}
Bulk E_F (above bulk CBM)	0.192 eV	0.510 eV
Surface sheet density	6.4×10^{13} cm^{-2}	5.9×10^{13} cm^{-2}
E_1(below E_F)	0.662 eV	0.797 eV
m^* at 1st subband minimum	$0.140m_0$	$0.161m_0$
E_2(below E_F)	0.233 eV	0.511 eV
m^* at 2nd subband minimum	$0.080m_0$	$0.120m_0$

bands. However, the fundamental difference between the two data sets is the energy of the subband minima. This difference is directly related to the charge density in the conduction band. Recall the surface for the data in Fig. 2 was prepared by simply annealing in UHV, while that for Fig. 3 was prepared by two cycles of N_2^+ bombardment and UHV annealing. Clearly, the latter method of surface preparation leads to a higher density of charge donors, most likely N vacancies. It is interesting to consider whether the increase in the charge occurs in the bulk conduction band, or in the quantum well states of the accumulation layer. If it is the latter, then E_F rises simply through the increased population of the quantum well states, defined by a potential barrier that remains static as the surface treatment changes. However, if the surface treatment leads to a change in the potential due to an increase in the population of the bulk conduction band, then the quantum well states must also change. Consequently, the increase in separation between E_F and the subband minima could arise from a narrowing of the electron accumulation layer, but leaving the charge density in the accumulation layer essentially constant. Analysis of the subband minima in Figs. 2 and 3 using the method discussed above leads to the results presented in Table I. This analysis suggests that it is the potential and not the electron density that is varying.

Finally, the structure of the Fermi surface and constant binding energy contours provide important information on the nature of the quantum well states. Two characteristics of the data in Fig. 4 are of importance: (i) the Fermi surface is circular, but the 0.5 eV energy contour displays a hexagonal symmetry, and (ii) the outer band forms a well-defined contour, but the inner band exhibits quite diffuse emission. We consider the origin of the first observation to be a consequence of the structure of the conduction band. While the electron energy and momentum in the accumulation layer is quantized perpendicular to the surface due to the potential well, the energy and momentum parallel to the surface remains determined by the bulk crystal potential. Examination of the calculated band structure shows that a constant energy cut through the conduction band at E_F generates a circular Fermi surface such as measured in Fig. 4(a), while a cut at 0.5 eV below E_F generates a noncircular structure. The orientation of the hexagonal structure in Fig. 4(c) is identical to that of the measured hexagonal LEED pattern, which reflects the surface unit cell symmetry. Calculated constant energy contours are required for further analysis of this result. It is possible that the origin of the diffuse ARPES signal associated with the inner band in Fig. 2 and lies in structural disorder near the sample surface. Electrons closest to E_F, and with the smallest momentum, are the most likely to scatter from defects or from disorder at the vacuum/solid interface.

In summary, the electronic structure of the accumulation layer in InN has been measured using ARPES. The electrons in the layer have been found to exist in discrete quantum well states, defined perpendicular to the film surface. The binding energy of the states is in excellent agreement with theory. The states display nonparabolic dispersion near Γ. The Fermi surfaces of these states have also been measured. Finally, the trapping potential has been shown to depend on the method of surface processing, allowing the structure of the quantum well states to be controlled.

This work was supported in part by the NSF under Grant No. DMR-0311792, by the ARO under Grant No. 40126-PH, and by the AFOSR. The NSLS is supported by the DOE, Division of Materials and Chemical Sciences, and the ALS by the DOE, Materials Sciences Division under Contract No. DE-AC03-76SF00098. The authors thank Antonio Castro-Neto for helpful discussions.

*Corresponding author.
Electronic address: ksmith@bu.edu

[1] F. A. Ponce and D. P. Bour, Nature (London) **386**, 351 (1997).
[2] J. Wu *et al.*, Appl. Phys. Lett. **80**, 3967 (2002).
[3] J. Wu *et al.*, Appl. Phys. Lett. **80**, 4741 (2002).
[4] I. Mahboob, T. D. Veal, L. F. J. Piper, C. F. McConville, H. Lu, W. J. Schaff, J. Furthmuller, and F. Bechstedt, Phys. Rev. B **69**, 201307 (2004).
[5] I. Mahboob, T. D. Veal, C. F. McConville, H. Lu, and W. J. Schaff, Phys. Rev. Lett. **92**, 036804 (2004).
[6] H. Lu *et al.*, Appl. Phys. Lett. **82**, 1736 (2003).
[7] K. A. Rickert *et al.*, Appl. Phys. Lett. **82**, 3254 (2003).
[8] T. D. Veal, L. F. J. Piper, M. R. Phillips, M. H. Zareie, H. Lu, W. J. Schaff, and C. F. McConville, Phys. Status Solidi A **203**, 85 (2006).
[9] T. P. Chen, C. Thomidis, J. Abell, W. Li, and T. D. Moustakas, J. Cryst. Growth **288**, 254 (2006).
[10] T. Hofmann *et al.*, Phys. Status Solidi C **3**, 1854 (2006).
[11] L. O. Olsson *et al.*, Phys. Rev. Lett. **76**, 3626 (1996).
[12] C. Stampfl *et al.*, Phys. Rev. B **61**, R7846 (2000).
[13] H. Ubensee *et al.*, Phys. Status Solidi B **147**, 823 (1988).
[14] B. R. Nag, *Electron Transport in Compoundsemiconductors* (Springer-Verlag, Berlin, 1980); J. Wu *et al.*, Phys. Rev. B **66**, 201403 (2002).
[15] C. B. Duke, Phys. Rev. **159**, 632 (1967); Phys. Rev. **164**, 1214 (1967); Phys. Rev. **177**, 1394 (1969).
[16] R. E. Jones *et al.*, Phys. Rev. Lett. **96**, 125505 (2006).